Analyzing the effects of thermal stress on insulator papers by solid-state ^{13}C NMR spectroscopy

Paul Jusner[1], Markus Bacher[1], Jonas Simon[1], Florian Bausch[1], Hajar Khaliliyan[1], Sonja Schiehser[1], Ivan Sumerskii[2], Elisabeth Schwaiger[3], Antje Potthast[1], Thomas Rosenau[1,4]

[1] Department of Chemistry, Institute of Chemistry of Renewable Resources, University of Natural Resources and Life Sciences Vienna (BOKU), Konrad-Lorenz-Straße 24, A-3430 Tulln, Austria

[2] Core Facility Analysis of Lignocellulosics, University of Natural Resources and Life Sciences Vienna (BOKU), Konrad-Lorenz-Straße 24, A-3430 Tulln, Austria

[3] Mondi Frantschach GmbH, Frantschach 5, A-9413 St. Gertraud, Austria

[4] Johan Gadolin Process Chemistry Centre, Åbo Akademi University, Porthansgatan 3, FI-20500 Åbo/Turku, Finland

Supplementary information

Table of content

List of figures

List of tables

List of formulas

1. “Peak Analyzer” settings in OriginPro 2020

For deconvolution of the C4 resonance (79 to 91 ppm) of ^{13}C CP/MAS NMR spectra, two distinct setups were implemented in the “Peak Analyzer” tool of OriginPro 2020 (OriginLab Corporation, USA). The softwood Kraft paper sample setup featured 8 peaks, whereas the setup for Whatman paper samples featured 7 peaks (no hemicelluloses signal). A constant baseline was set for each sample using the “minimum” mode. The maximum number of iterations was set to 500 at a tolerance value of $1 * 10^{(-4)}$. Negative ordinate peak values were excluded.

Peak positions (ppm) and shapes (Wickholm *et al*., 1998, Zuckerstätter *et al*., 2013):

P1 = 89.4, Lorentz (Iα)

P2 = 88.8, Lorentz (Iαβ)

P3 = 88.5, Gaussian (PC)

P4 = 88.0, Lorentz (Iβ)

P5 = 84.2, Gaussian (AS I)

P6 = 83.9, Gaussian (IAS)

P7 = 83.2, Gaussian (AS II)

P8 = 81.7, Gaussian (HC)

Fit control peak constraints:

w = FWHH (ppm) ±3 * SD from Wickholm *et al*. (1998)

A = peak area

A__2=A__1+A__4;

A__1<A__4;

A__8<A__6;

0.11<w__1<0.76;

0.34<w__2<0.58;

1.40<w__3<1.94;

0.30<w__4<1.31;

0.22<w__5<1.17;

2.54<w__6<5.17;

0.29<w__7<0.76;

0.55<w__8<1.86;

2. ^{13}C CP/MAS NMR results of Whatman paper No. 1 (WP) ageing series

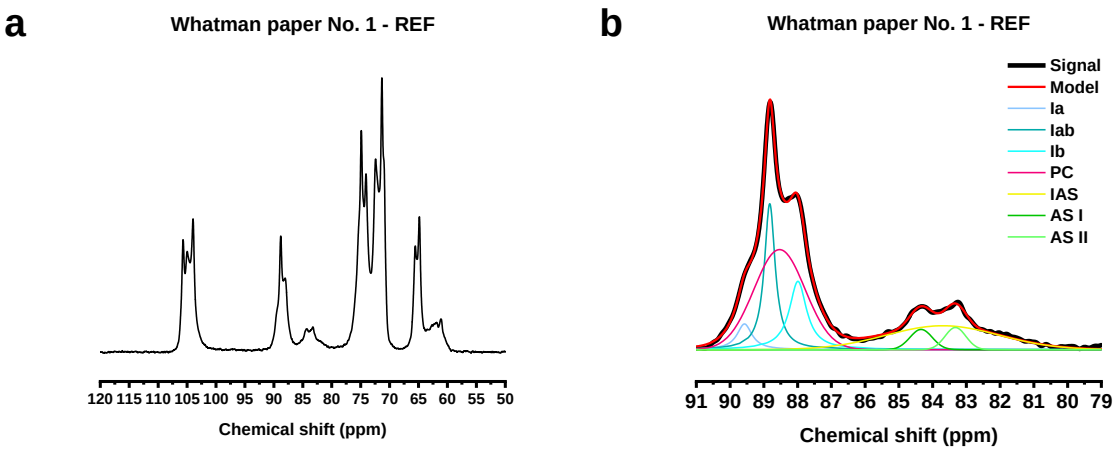

Figure S1: ^{13}C CP/MAS NMR spectrum of WP_{REF} (**a**) and deconvoluted C4 resonance (**b**).

Table S1: Peak properties of C4 deconvolution (WP_{REF}).

WP REF	Shape	Relative intensity (%)	Position (ppm)	FWHH (ppm)
Iα	Lorentz	4.09	89.57	0.54
Iαβ	Lorentz	17.99	88.82	0.39
PC	Gaussian	36.64	88.53	1.79
Iβ	Lorentz	13.61	87.99	0.64
AS I	Gaussian	3.90	84.34	0.85
IAS	Gaussian	20.37	83.70	4.06
AS II	Gaussian	3.39	83.32	0.70

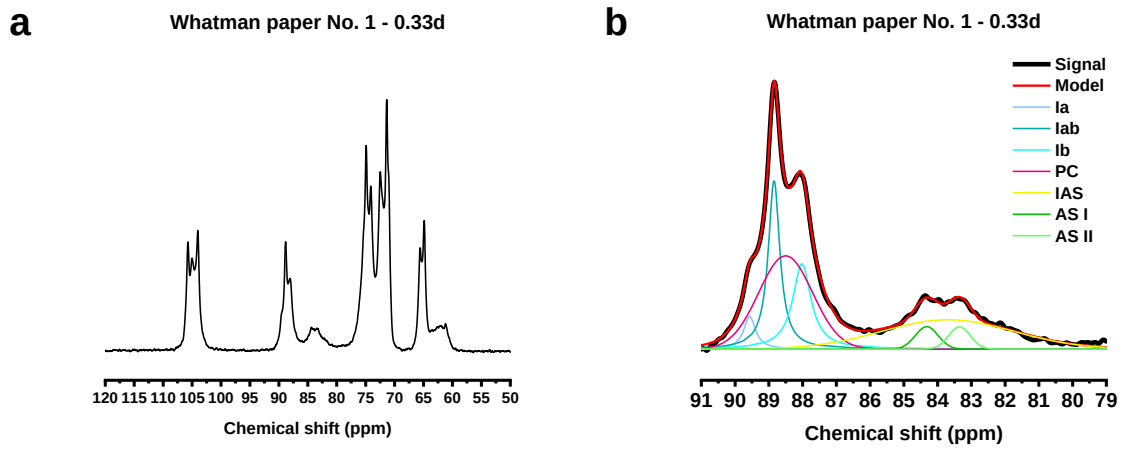

Figure S2: ^{13}C CP/MAS NMR spectrum of $WP_{0.33d}$ (**a**) and deconvoluted C4 resonance (**b**).

Table S2: Peak properties of C4 deconvolution ($WP_{0.33d}$).

WP 0.33d	Shape	Relative intensity (%)	Position (ppm)	FWHH (ppm)
Iα	Lorentz	3.56	89.57	0.42
Iαβ	Lorentz	18.28	88.85	0.41
PC	Gaussian	32.38	88.50	1.88
Iβ	Lorentz	14.52	88.02	0.65
AS I	Gaussian	3.31	84.32	0.80
IAS	Gaussian	24.83	83.70	4.61
AS II	Gaussian	3.11	83.35	0.76

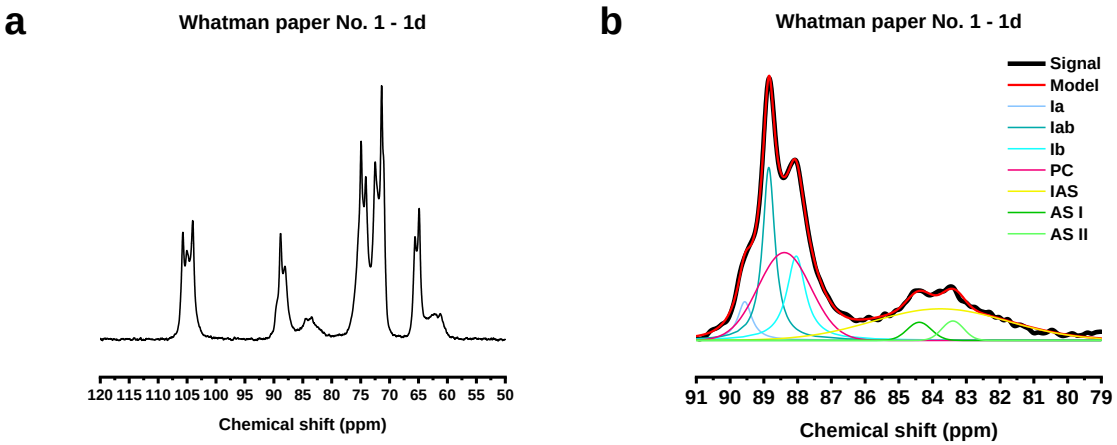

Figure S3: ^{13}C CP/MAS NMR spectrum of WP_{1d} (**a**) and deconvoluted C4 resonance (**b**).

Table S3: Peak properties of C4 deconvolution (WP_{1d}).

WP 1d	Shape	Relative intensity (%)	Position (ppm)	FWHH (ppm)
Iβ	Lorentz	4.88	89.56	0.50
Iαβ	Lorentz	19.40	88.85	0.44
PC	Gaussian	29.30	88.39	1.84
Iβ	Lorentz	14.27	88.04	0.66
AS I	Gaussian	2.75	84.39	0.84
IAS	Gaussian	26.73	83.77	4.72
AS II	Gaussian	2.67	83.40	0.76

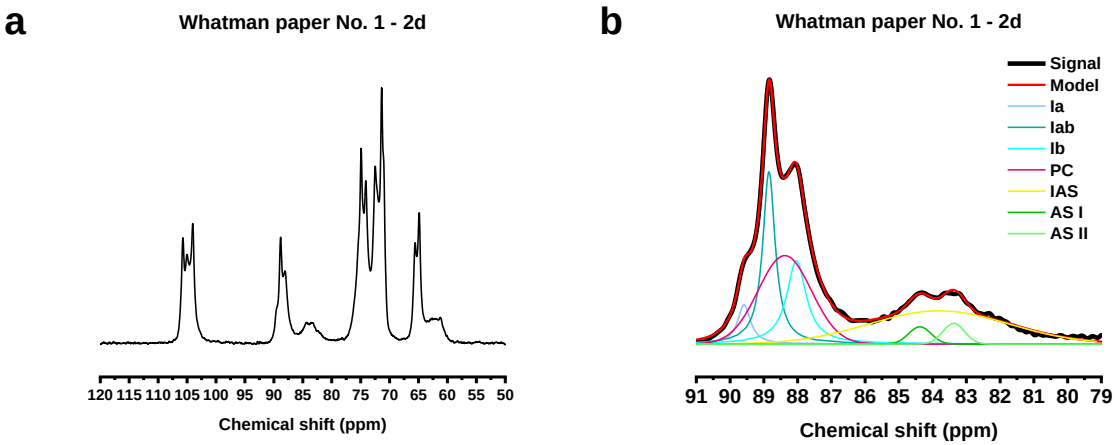

Figure S4: ^{13}C CP/MAS NMR spectrum of WP_{2d} (**a**) and deconvoluted C4 resonance (**b**).

Table S4: Peak properties of C4 deconvolution (WP_{2d}).

WP 2d	Shape	Relative intensity (%)	Position (ppm)	FWHH (ppm)
Iα	Lorentz	4.43	89.59	0.46
Iαβ	Lorentz	19.01	88.85	0.44
PC	Gaussian	28.90	88.38	1.86
Iβ	Lorentz	14.34	88.03	0.70
AS I	Gaussian	2.36	84.38	0.78
IAS	Gaussian	28.20	83.81	4.87
AS II	Gaussian	2.76	83.37	0.76

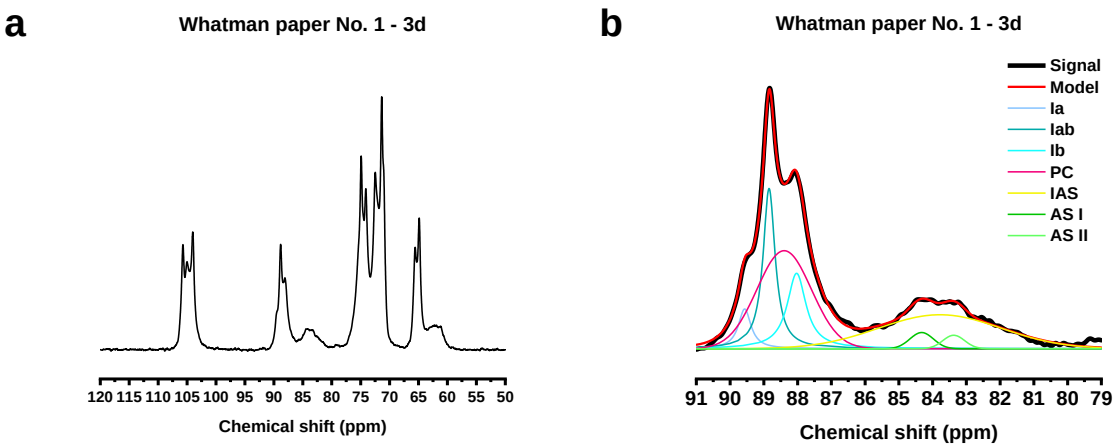

Figure S5: ^{13}C CP/MAS NMR spectrum of WP_{3d} (**a**) and deconvoluted C4 resonance (**b**).

Table S5: Peak properties of C4 deconvolution (WP_{3d}).

WP 3d	Shape	Relative intensity (%)	Position (ppm)	FWHH (ppm)
Iα	Lorentz	4.55	89.57	0.45
Iαβ	Lorentz	17.75	88.84	0.43
PC	Gaussian	34.02	88.40	1.90
Iβ	Lorentz	12.98	88.03	0.67
AS I	Gaussian	2.43	84.32	0.82
IAS	Gaussian	26.40	83.79	4.27
AS II	Gaussian	1.87	83.37	0.76

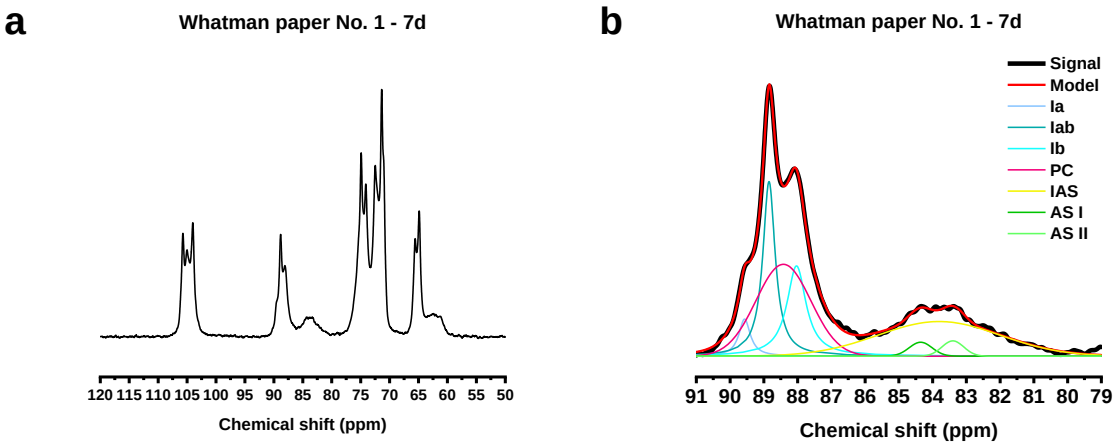

Figure S6: ^{13}C CP/MAS NMR spectrum of WP_{7d} (**a**) and deconvoluted C4 resonance (**b**).

Table S6: Peak properties of C4 deconvolution (WP_{7d}).

WP 7d	Shape	Relative intensity (%)	Position (ppm)	FWHH (ppm)
Iα	Lorentz	3.77	89.57	0.41
Iαβ	Lorentz	19.33	88.85	0.44
PC	Gaussian	31.23	88.42	1.91
Iβ	Lorentz	15.36	88.03	0.68
AS I	Gaussian	1.99	84.35	0.80
IAS	Gaussian	26.24	83.81	4.27
AS II	Gaussian	2.07	83.40	0.76

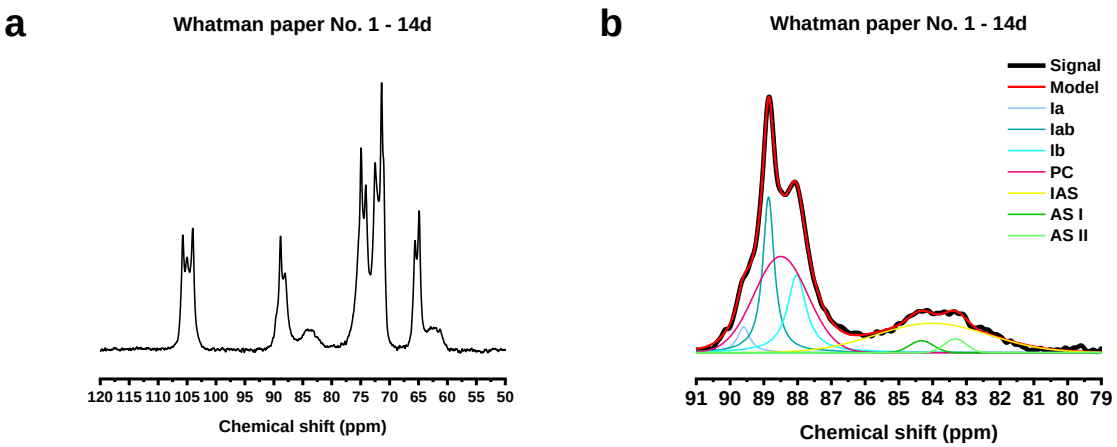

Figure S7: ^{13}C CP/MAS NMR spectrum of WP_{14d} (**a**) and deconvoluted C4 resonance (**b**).

Table S7: Peak properties of C4 deconvolution (WP_{14d}).

WP 14d	Shape	Relative intensity (%)	Position (ppm)	FWHH (ppm)
Iα	Lorentz	3.23	89.60	0.45
Iαβ	Lorentz	18.20	88.86	0.41
PC	Gaussian	36.29	88.50	1.87
Iβ	Lorentz	14.73	88.03	0.67
AS I	Gaussian	2.00	84.33	0.83
IAS	Gaussian	23.43	84.01	3.96
AS II	Gaussian	2.12	83.33	0.76

3. ^{13}C CP/MAS NMR results of softwood Kraft paper (SWKP) ageing series

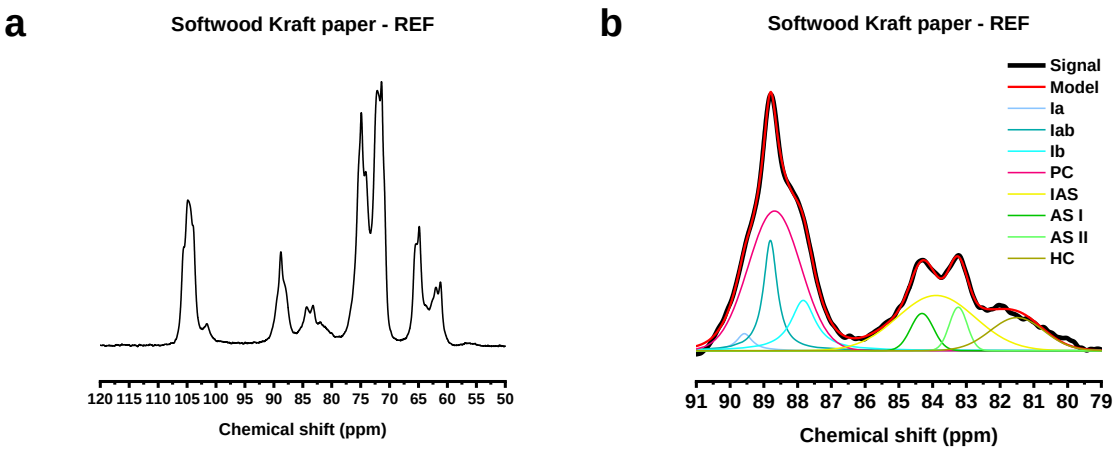

Figure S8: ^{13}C CP/MAS NMR spectrum of $SWKP_{REF}$ (**a**) and deconvoluted C4 resonance (**b**).

Table S8: Peak properties of C4 deconvolution ($SWKP_{REF}$).

SWKP REF	Shape	Relative intensity (%)	Position (ppm)	FWHH (ppm)
Iα	Lorentz	1.94	89.58	0.56
Iαβ	Lorentz	11.26	88.81	0.49
PC	Gaussian	38.00	88.68	1.84
Iβ	Lorentz	9.10	87.83	0.88
AS I	Gaussian	4.38	84.31	0.79
IAS	Gaussian	22.17	83.90	2.71
AS II	Gaussian	4.02	83.24	0.62
HC	Gaussian	9.13	81.50	1.86

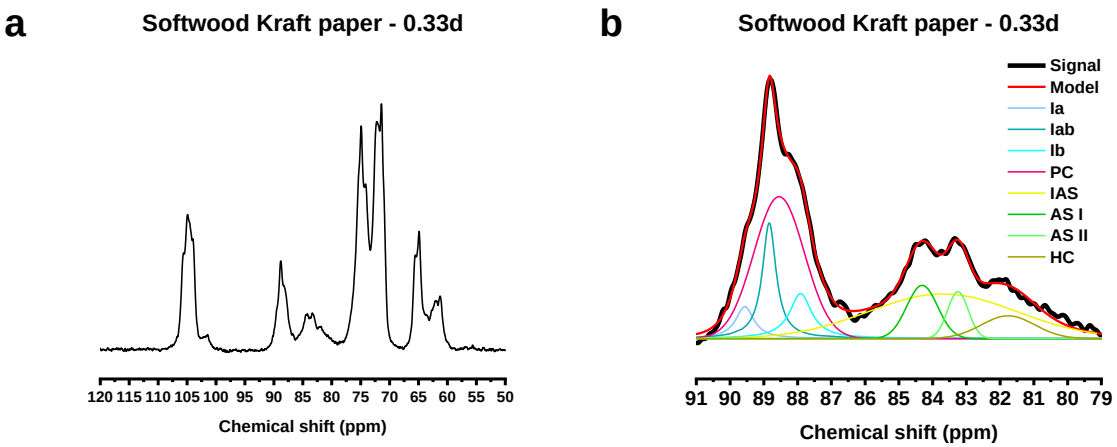

Figure S9: ^{13}C CP/MAS NMR spectrum of $SWKP_{0.33d}$ (**a**) and deconvoluted C4 resonance (**b**).

Table S9: Peak properties of C4 deconvolution ($SWKP_{0.33d}$).

SWKP 0.33d	Shape	Relative intensity (%)	Position (ppm)	FWHH (ppm)
Iα	Lorentz	3.69	89.56	0.65
Iαβ	Lorentz	10.37	88.84	0.49
PC	Gaussian	32.52	88.55	1.76
Iβ	Lorentz	6.45	87.91	0.79
AS I	Gaussian	7.47	84.31	1.08
IAS	Gaussian	29.56	83.70	5.17
AS II	Gaussian	4.42	83.25	0.73
HC	Gaussian	5.52	81.76	1.86

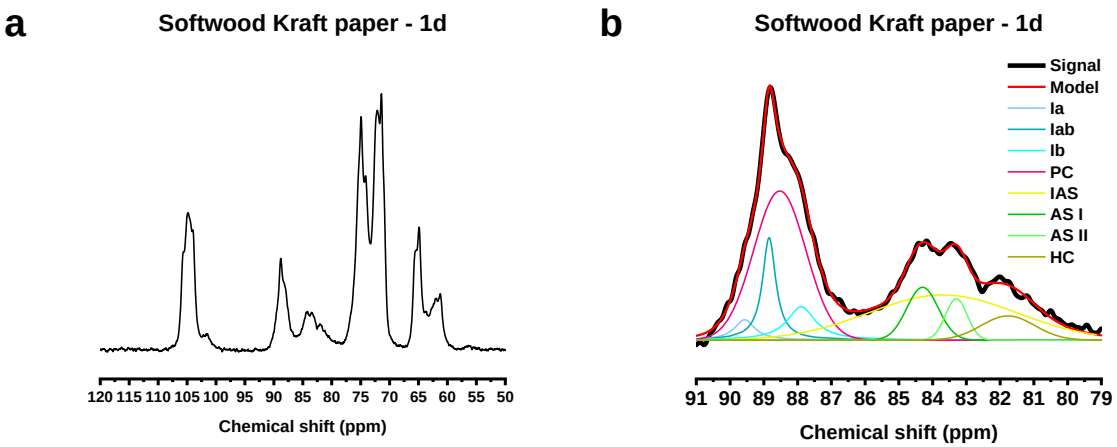

Figure S10: ^{13}C CP/MAS NMR spectrum of $SWKP_{1d}$ (**a**) and deconvoluted C4 resonance (**b**).

Table S10: Peak properties of C4 deconvolution ($SWKP_{1d}$).

SWKP 1d	Shape	Relative intensity (%)	Position (ppm)	FWHH (ppm)
Iα	Lorentz	2.60	89.57	0.73
Iαβ	Lorentz	8.90	88.84	0.47
PC	Gaussian	35.19	88.53	1.82
Iβ	Lorentz	5.98	87.89	1.00
AS I	Gaussian	7.56	84.30	1.10
IAS	Gaussian	29.83	83.70	5.17
AS II	Gaussian	4.08	83.30	0.76
HC	Gaussian	5.86	81.77	1.86

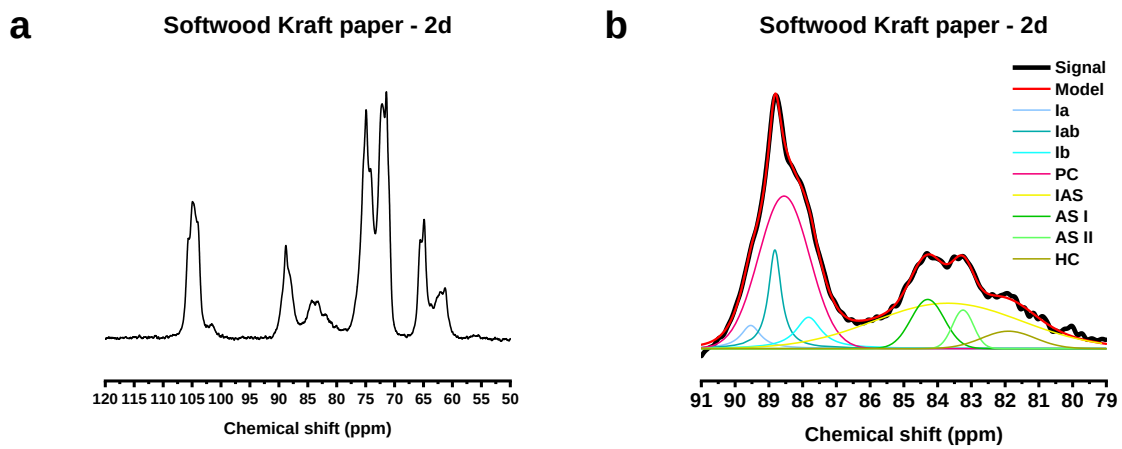

Figure S11: ^{13}C CP/MAS NMR spectrum of $SWKP_{2d}$ (**a**) and deconvoluted C4 resonance (**b**).

Table S11: Peak properties of C4 deconvolution ($SWKP_{2d}$).

SWKP 2d	Shape	Relative intensity (%)	Position (ppm)	FWHH (ppm)
Iα	Lorentz	2.97	89.54	0.71
Iαβ	Lorentz	8.52	88.82	0.45
PC	Gaussian	36.44	88.55	1.78
Iβ	Lorentz	5.28	87.82	0.91
AS I	Gaussian	7.66	84.29	1.16
IAS	Gaussian	30.99	83.70	5.17
AS II	Gaussian	3.79	83.25	0.73
HC	Gaussian	4.35	81.90	1.86

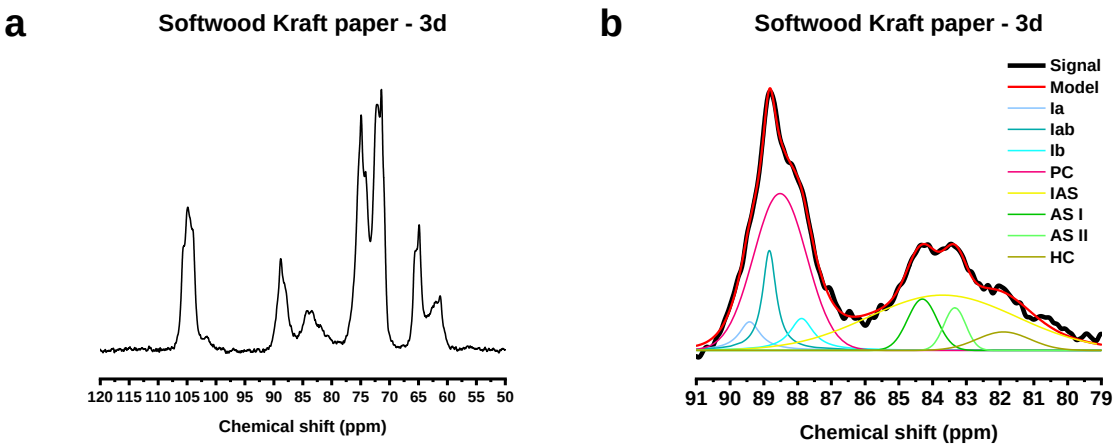

Figure S12: ^{13}C CP/MAS NMR spectrum of $SWKP_{3d}$ (**a**) and deconvoluted C4 resonance (**b**).

Table S12: Peak properties of C4 deconvolution ($SWKP_{3d}$).

SWKP 3d	Shape	Relative intensity (%)	Position (ppm)	FWHH (ppm)
Iα	Lorentz	3.55	89.42	0.76
Iαβ	Lorentz	8.30	88.84	0.49
PC	Gaussian	35.09	88.52	1.85
Iβ	Lorentz	4.51	87.88	0.84
AS I	Gaussian	6.40	84.30	1.03
IAS	Gaussian	34.07	83.70	5.17
AS II	Gaussian	3.92	83.34	0.76
HC	Gaussian	4.16	81.90	1.86

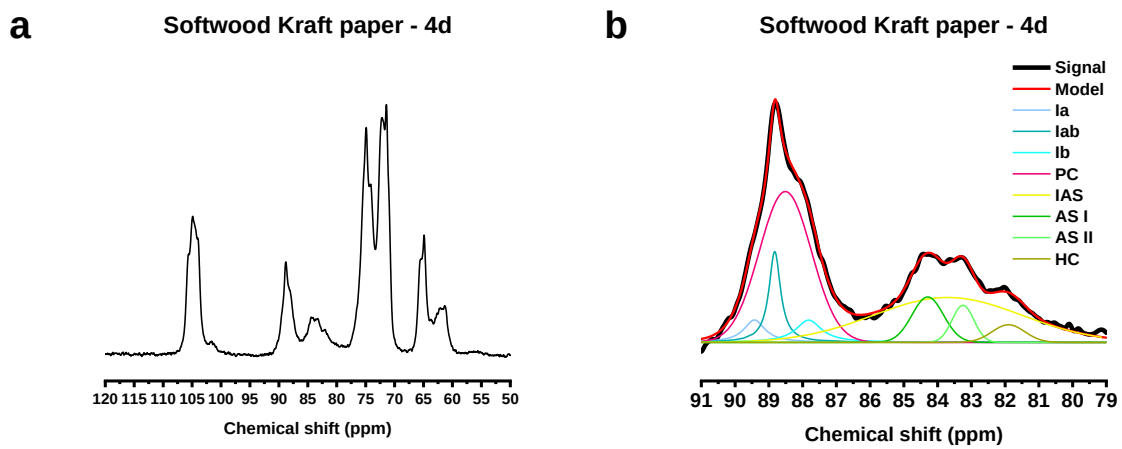

Figure S13: ^{13}C CP/MAS NMR spectrum of SWKP$_{4d}$ (**a**) and deconvoluted C4 resonance (**b**).

Table S13: Peak properties of C4 deconvolution (SWKP$_{4d}$).

SWKP 4d	Shape	Relative intensity (%)	Position (ppm)	FWHH (ppm)
Iα	Lorentz	3.23	89.43	0.75
Iαβ	Lorentz	7.56	88.83	0.41
PC	Gaussian	38.84	88.51	1.81
Iβ	Lorentz	4.04	87.82	0.92
AS I	Gaussian	7.08	84.29	1.10
IAS	Gaussian	32.41	83.70	5.17
AS II	Gaussian	4.00	83.25	0.76
HC	Gaussian	2.85	81.90	1.14

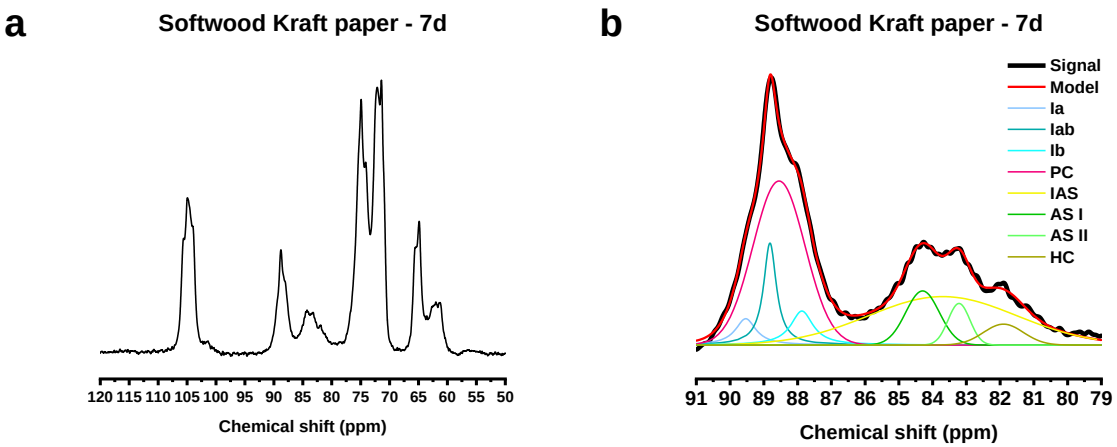

Figure S14: ^{13}C CP/MAS NMR spectrum of $SWKP_{7d}$ (**a**) and deconvoluted C4 resonance (**b**).

Table S14: Peak properties of C4 deconvolution ($SWKP_{7d}$).

SWKP 7d	Shape	Relative intensity (%)	Position (ppm)	FWHH (ppm)
Iα	Lorentz	3.27	89.54	0.74
Iαβ	Lorentz	8.24	88.82	0.46
PC	Gaussian	37.26	88.55	1.81
Iβ	Lorentz	4.73	87.87	0.79
AS I	Gaussian	7.95	84.30	1.17
IAS	Gaussian	30.93	83.70	5.17
AS II	Gaussian	3.97	83.22	0.76
HC	Gaussian	3.65	81.90	1.39

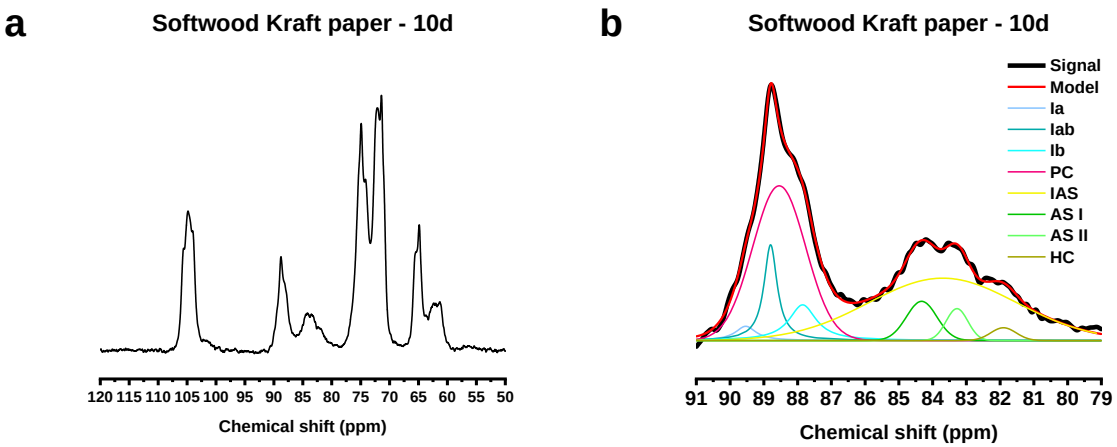

Figure S15: ^{13}C CP/MAS NMR spectrum of $SWKP_{10d}$ (**a**) and deconvoluted C4 resonance (**b**).

Table S15: Peak properties of C4 deconvolution ($SWKP_{10d}$).

SWKP 10d	Shape	Relative intensity (%)	Position (ppm)	FWHH (ppm)
Iα	Lorentz	1.76	89.54	0.74
Iαβ	Lorentz	7.93	88.80	0.47
PC	Gaussian	35.44	88.55	1.85
Iβ	Lorentz	5.92	87.85	0.97
AS I	Gaussian	5.17	84.32	1.06
IAS	Gaussian	39.37	83.70	5.17
AS II	Gaussian	3.01	83.28	0.76
HC	Gaussian	1.40	81.90	0.88

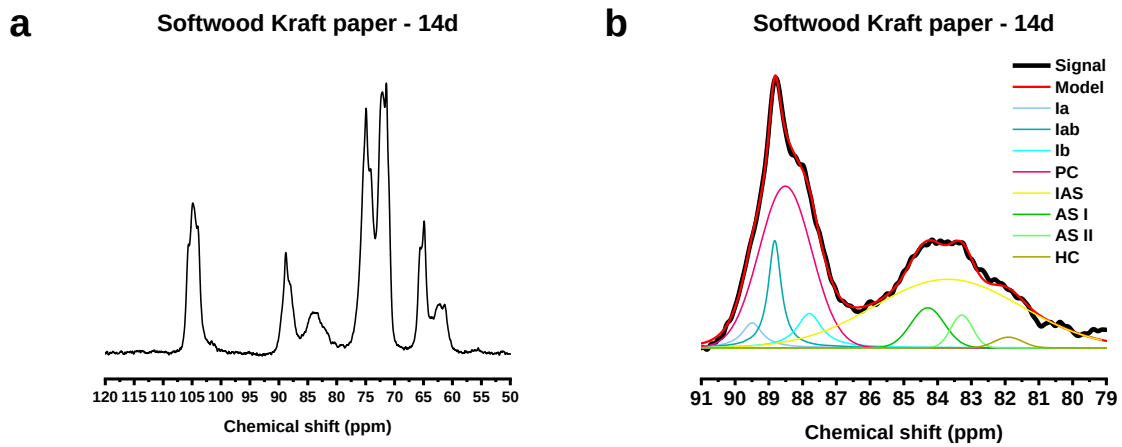

Figure S16: ^{13}C CP/MAS NMR spectrum of SWKP$_{14d}$ (**a**) and deconvoluted C4 resonance (**b**).

Table S16: Peak properties of C4 deconvolution (SWKP$_{14d}$).

SWKP 14d	Shape	Relative intensity (%)	Position (ppm)	FWHH (ppm)
Iα	Lorentz	2.87	89.49	0.73
Iαβ	Lorentz	8.09	88.82	0.46
PC	Gaussian	34.30	88.51	1.83
Iβ	Lorentz	4.97	87.80	0.90
AS I	Gaussian	5.44	84.29	1.17
IAS	Gaussian	40.25	83.70	5.14
AS II	Gaussian	2.88	83.28	0.76
HC	Gaussian	1.20	81.90	0.97

4. Calculation of lateral crystallite dimension

The lateral crystallite dimensions (LD) of the samples were calculated with formula (1) published by Newman (1999) by inserting crystallinity indices (CI) obtained from C4 deconvolution of ^{13}C CP/MAS NMR spectra and the average surface layer distance (d) of cellulose chains in a single crystallite.

(1) $$LD = (2 * d)/(1 - CI^{0,5})$$

$LD =$ lateral crystallite dimension

$d =$ average surface layer distance

$CI =$ crystallinity index

Newman compared wide angle x-ray scattering (WAXS) results for the LD of several samples with results calculated via formula (1) by inserting the CI from ^{13}C NMR spectra of the same samples and d derived from the 6 * 6 cellulose chain model (0.57 nm).

We calculated the LD of our samples based on d derived from the 24 cellulose chain crystallite model proposed by Oehme *et al*. (2015) (100 layer: 0.40 nm, 110 layer: 0.54 nm, 1-10 layer: 0.62, d: 0.52 nm). This is only an approximation, but when using the CIs determined by Newman via ^{13}C NMR and inserting d of the 24 chains model instead of d based on the 6 * 6 chain model, a better correlation of the original Newman-data with the WAXS results for LD

was found (*cf*. **Table S17** and **Figure S17**). Hence, we conclude that this is a valid approach for evaluating ^{13}C NMR data.

Table S17: LD and CI data published by Newman (1999) plus LD calculated based on the 24 chains model proposed by Oehme *et al*. (2015).

Sample	CI NMR	LD 6*6 chains	LD 24 chains	LD WAXS
Asplenium frond fibre	0.324	2.646	2.413	2.600
Sisal twine	0.435	3.348	3.053	3.000
Phormium leaf fibre	0.448	3.448	3.143	3.300
Cyathea frond fibre	0.450	3.463	3.158	3.100
Eucalyptus wood	0.488	3.782	3.448	3.500
Jute twine	0.489	3.791	3.456	3.400
Avicel powder	0.653	5.940	5.416	5.400
Linen sewing thread	0.661	6.097	5.559	5.600
Sigma C-6663 powder	0.771	9.349	8.524	7.900
Cotton fabric	0.777	9.618	8.770	7.800

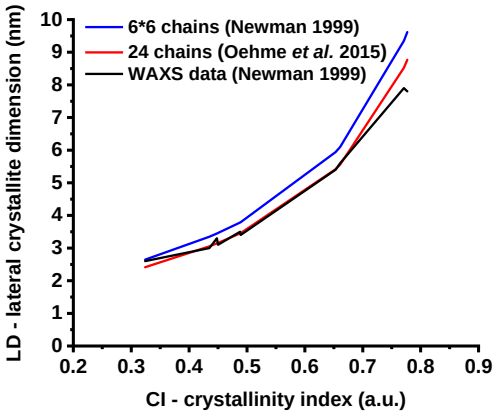

Figure S17: LD calculated with d based on the 6 * 6 model, LD calculated with d based on the 24 cellulose chains model, and LD obtained from WAXS measurements plotted against CI.

5. References

Newman, R. H. 1999. Estimation of the lateral dimensions of cellulose crystallites using 13C NMR signal strengths. *Solid State Nuclear Magnetic Resonance,* 15**,** 21-29.

Oehme, D. P., Downton, M. T., Doblin, M. S., Wagner, J., Gidley, M. J. & Bacic, A. 2015. Unique aspects of the structure and dynamics of elementary Iβ cellulose microfibrils revealed by computational simulations. *Plant Physiology,* 168**,** 3-17.

Wickholm, K., Larsson, P. T. & Iversen, T. 1998. Assignment of non-crystalline forms in cellulose I by CP/MAS 13C NMR spectroscopy. *Carbohydrate Research,* 312**,** 123-129.

Zuckerstätter, G., Terinte, N., Sixta, H. & Schuster, K. C. 2013. Novel insight into cellulose supramolecular structure through 13C CP-MAS NMR spectroscopy and paramagnetic relaxation enhancement. *Carbohydrate Polymers,* 93**,** 122-8.